Titanium implants with modified surfaces: Meta-analysis of in vivo osteointegration

Michael Gasik[a],

Annabel Braem[b],

Amol Chaudhari[c],

Joke Duyck[c],

Jozef Vleugels[b]

[a] Aalto University Foundation, School of Chemical Technology, P.O. Box 16200, FIN-00076 AALTO, Finland

[b] Department of Metallurgy and Materials Engineering, KU Leuven, Kasteelpark Arenberg 44, B-3001 Heverlee, Belgium

[c] Department of Prosthetic Dentistry, BIOMAT Research Cluster, KU Leuven, Kapucijnenvoer 7a, B-3000 Leuven, Belgium

Received 6 October 2013, Revised 3 December 2014, Accepted 22 December 2014, Available online 24 December 2014

doi:10.1016/j.msec.2014.12.074

Highlights

- Various titanium specimens were studied in vivo on osteointegration vs their properties.
- Non-porous implants had a better performance when coated with bioactive glass.
- Porous implants have shown the best results for hydrothermally treated specimens.
- Good correlation was found with the previous in vitro tests.
- New analysis of the in vivo data has shown benefits to assess biomaterials performance.

Abstract

Titanium-based implants are widely used in modern clinical practice, but their “optimal” properties in terms of porosity and topology, roughness and hydrophilic parameters are being a subject of intensive discussions. Recent in vitro results have shown a possibility to optimize the surface of an implant with maximal repelling of bacteria (Staphylococcus aureus, Staphylococcus epidermidis) and

improvement in human osteogenic and endothelial cell adhesion, proliferation and differentiation. In this work, these different grades titanium implants were tested in vivo using the same analytical methodology. In addition to material parameters, key histomorphometrical parameters such a regeneration area, bone adaptation area and bone-to-implant contact were determined after 2 and 4 weeks of implantation in rabbit animal model. Porous implants have more clear differences than non-porous ones, with the best optimum values obtained on hydrothermally treated electrophoretically deposited titanium. These in vivo data correlate well with the optimal prediction made by in vitro tests.

Keywords

Titanium;

Surface;

Histomorphometry;

Osteointegration;

Bone;

Data analysis

---

1. Introduction

Titanium implants are widely used in modern clinical practice especially in load-bearing applications such as orthopedic and dental implants. Many producers are developing various grades of implants, with the modern trend on surface modification. All titanium implants might be roughly divided into ones with porous surface (normally coating such as vacuum plasma sprayed (VPS) titanium) and without (polished, sandblasted, etched or otherwise treated). Furthermore, any of this type may be additionally coated with an external layer (hydroxyapatite, bioactive glass, etc.) and it is of a general knowledge that such modification would affect surface roughness, porosity, wettability and consequently cell and bacterial adhesion to the implant. Together with biomechanical factors, these set conditions for bone in-growth and osteointegration. Although the process is generally well understood, many links between input (surface characteristics, coatings) and output (bone to implant contact, etc.) parameters are only qualitatively known. It is difficult to make a vast number of specific surfaces with different features being independently varied to evaluate their specific effect in vivo. It was recently demonstrated in vitro to be possible to adjust titanium coating parameters to reduce bacterial adhesion and to enhance cell proliferation and differentiation at the same time vs. non-optimized plasma-sprayed Ti [1]. These data, however, might not be directly extrapolated to in vivo host conditions, as there are many other variables, most of them are beyond control (such as specific animal mobility or its health conditions). Thus, in vivo results are more difficult to quantify and whether such quantification is made, the scatter in the data is rather significant to accept or decline a particular test specimen.

Such post-analysis of the data is often limited to very simple (ANOVA) methods for single hypotheses. This is difficult to apply to scattered data with linked variables (and when their error distribution is unknown). The FDA guidelines recommend Bayesian methods for planning and evaluation (docket No. 2006D-0191) instead of simple statistics, which might affect the likelihood function and bias the output. However, it is still quite common to see conclusions based just on p-values in many reports [2] and [3]. Taking into account the variety of the factors, it is not straightforward to find out the

“real” links between the implanted specimen properties and in vivo output. For example, what is the relevance of in vivo studies using a proximal tibia where the extracted implant (cylinder) is mechanically loaded and the push-out force is recorded [4], [5], [6] and [7]. Despite its simplicity, this test often produces inadequate results: the knowledge on the implant push-out resilience of example ~ 370 J makes little sense when the standard deviation on this value is ± 480 J. When tibia/femur being histologically examined, every implant commonly displays differences in bone in-growth. The cylinder main axis is not always perpendicular to the bone surface (as assumed by the test protocol), and thus stresses or energy measurements might be misleading (even negative values might be obtained due to uneven deformation, misalignment and non-uniformity of residual stresses). Some cortical bone might be delaminated or over-dried before the test and there are no data about the influence of parameters on osteointegration if it is being measured in this way. The basic simulations of this procedure [4] have confirmed these variations together with scatter in the test rig tool parameters often lead to non-interpretable test results.

The advanced meta-analytical methods and Bayesian statistics, applied to the design of experiments and output data, have an improved ability to determine the relative influence of different parameters on a given phenomenon, to find existing relationships among the considered variables, to resolve the unavoidable noise present within a vast set of numerical data. The challenge of meta-analysis application to implants testing is to overcome limitations due to a considerable amount of time needed to perform an analysis, when the number of parameters is very high and when they are linked with each other and with the output functions in an unknown or a non-quantified way [8], [9], [10], [11] and [12]. The common definition of meta-analysis assumes it as a collection of techniques for a systematic review of the relevant literature used in reaching an overall estimate of effect size, despite some criticism due to difficulties of knowing which data should be included and to which population final results actually apply [11] and [12].

In this work, we are rather analyzing the effect of different titanium implants and their surface parameters linked with histomorphometrical features obtained from in vivo tests, for the same materials which behavior in vitro has been recently reported [1]. The main essential feature of advanced meta-analytical methods applied to the subject of the study is in focusing on the links between the controllable input variables (material parameters) and in vivo responses, without speculating about the exact mechanisms behind these interactions. For such complex tasks involving many cross-linked interactions, meta-analytical methods have proven to provide answers and correct predictions with meta-modeling and multi-variate analysis [9], [13], [14] and [15]. It is noteworthy that here meta-analytical methods are specifically related to meta-modeling and multi-variate approaches [8] and [9], and not to the conventional meta-analysis as commonly used [11] and [12]. Thus here no usual data search is made but rather the similar method is applied to the set of generated experimental data. Due to this, for instance, standard meta-analytical plots [11] and [12] are not always possible or relevant, although some results like distribution, confidence intervals and outliers still could have sense.

2. Materials and methods

2.1. Implants

Implant design was as described in [16]: commercially pure Ti sheets (grade 2, thickness 1 mm, Goodfellow, UK), were laser-cut into Ø 4 mm discs and etched in a HF:HNO3 = 1:5 solution (specimens marked as “etched”). After autoclave sterilization, these discs were used both as substrate material and as the reference material for the in vivo tests. Additionally, the etched titanium surface was modified by seven different experimental coatings (Table 1).

Table 1.

Key parameters of the various implant materials. Values represent average ± standard deviations, except for IPC where minimum, mean and maximum sizes are given.

Sample	Sa	Sz	Str	Sdr	Wetting angle	Porosity	IPC (low)	IPC (high)	IPC (mean)
	(µm)	(µm)	(−)	(%)	(°)	(%)	(µm)	(µm)	(µm)
Etched cp Ti	0.32 ± 0.03	4.00 ± 0.78	0.56 ± 0.10	0.39 ± 0.04	73.0 ± 8.1	0	0	0	0
Anodised cp Ti	0.33 ± 0.05	4.12 ± 0.84	0.53 ± 0.12	0.40 ± 0.04	46.5 ± 10.8	0	0	0	0
Anodised cp Ti → MBAG	3.18 ± 0.43	32.73 ± 8.00	0.73 ± 0.16	94.01 ± 25.22	0	0	0	0	0
EPD Ti (P)	4.48 ± 0.37	50.73 ± 1.83	0.64 ± 0.13	61.71 ± 15.41	102.2 ± 3.4	51.2 ± 3.9	2	50	7
EPD Ti (P_Vm)	7.95 ± 0.68	103.80 ± 12.46	0.70 ± 0.07	218.96 ± 41.39	105.7 ± 7.2	65.2 ± 3.2	2	150	10
EPD Ti (P) → HT	4.93 ± 1.95	67.24 ± 22.08	0.67 ± 0.14	56.87 ± 27.20	0	45.9 ± 1.0	2	50	7
EPD Ti (P) → MAO	4.30 ± 0.24	51.67 ± 7.73	0.75 ± 0.12	35.59 ± 9.85	0	28.0 ± 3.8	0.2	15	5
EPD Ti (P) → SGBAG	4.26 ± 1.62	60.75 ± 11.46	0.79 ± 0.06	40.49 ± 11.11	0	51.3 ± 3.4	1	30	5

Sa — arithmetical mean height of the surface; Sz — ten point height, average height of the 5 highest and 5 lowest points; Str — texture aspect ratio: > 0.5 means isotropic, < 0.3 indicates directionality; Sdr — developed area ratio: percentage of additional surface area as compared to an ideal plane the size of the sampling area.

Firstly, anodic oxidation was used to increase the thickness of the natural TiO2 oxide layer from 15 nm to about 60 nm (this material is named “anodized”). Next, a melt-derived bioactive glass–ceramic coating (50.1 wt.% SiO2, 25.2 CaO, 20.1 Na2O and 4.6 P2O5, thickness ~ 10 µm) was applied on the anodized cp Ti substrate by dipping in a bioactive glass powder suspension followed by 30 min sintering at 800 °C in vacuum (specimens marked as “MBAG”). Porous pure Ti coatings were manufactured using electrophoretic deposition (EPD) of a TiH2 powder suspension or a combination of a suspension and emulsion followed by dehydrogenation (500–550 °C) and vacuum sintering (850 °C), as described in [17], [18] and [19]. Distinct TiH2 powder grades of different particle sizes, all supplied by Chemetall GmbH (Germany), have been used: grade type P (average particle size 8.0 ± 2.0 µm, maximal 60 µm), U (5.0 ± 1.0 µm, maximal 45 µm) and VM (1.8 ± 0.2 µm, maximal 45 µm). Different pore size and morphologies were realized by combining various particle sizes [1].

These coatings of EPD Ti are denominated “P” and “P_Vm” respectively, hereby referring to the starting powder grades. In addition, three different functionalizing coatings have been applied to EPD Ti (P). Chemical modification without altering the roughness or pore structure was done by a hydrothermal treatment (Jožef Stefan Institute, Slovenia) to apply a nanometer thin anatase TiO2 layer [20], specimens marked as “HT”. The micro-arc oxidation (MAO, University of Bayreuth, Germany) was performed at 150 V in a 1 M H3PO4 solution with hydroxyapatite and CaCl2 additions, was used to produce a pore-filling TiO2 layer containing Ca2 + and PO43 − ions [21], specimens marked as “MAO”. Finally a bioactive glass–ceramic coating (60 wt.% SiO2, 20 CaO, 15 Na2O and 5 P2O5, thickness ~ 1 µm) was applied on the internal surface of the EPD Ti (P) coating using an all-alkoxide sol–gel synthesis [22], specimens denominated as “SGBAG” (note that MBAG above and SGBAG bioactive glasses have different compositions).

Prior to implantation, all samples were steam sterilized in an autoclave (20 min, 121 °C) except for the anodized MBAG, MAO and SGBAG specimens, which were heated to 200 °C in a vacuum furnace to avoid dissolution of the functionalized coatings.

2.2. Surface and bulk characterization

Surface and pore structure of the various coatings was analyzed as described in [1]. Surface roughness was measured by white light interferometry (Wyko NT 3300 Optical Profiler, Veeco Metrology Inc., USA). An average of 10 point measurements was taken. The roughness data were quantitatively processed using MountainsMapH Premium software (Digital Surf, France). According to the guidelines for the topographic evaluation of implant surfaces suggested in [23], the average roughness and ten-points height (Sa and Sz, amplitude parameters), texture aspect ratio (Str, spatial parameter) and developed interfacial area ratio (Sdr, hybrid parameter) are presented in Table 1. Water contact angles were measured by sessile drop tests using optical imaging (CaM200, KSV, USA), averaging for ten measurements (Table 1). Pore characteristics were investigated by image analysis (PPM2OOF software, NIST, USA; and µCT-analyser, SkyScan, Belgium) in combination with mercury intrusion porosimetry (AutoPore IV 9500, Micromeritics, Germany). Total porosity was determined by image analysis of backscattered electron images obtained by scanning electron microscopy (SEM XL30-FEG, FEI, The Netherlands) of representative metallographic cross-sections, while mercury porosimetry was used to assess the minimal, mean and maximal interconnecting pore channel (IPC) sizes.

2.3. Surgical procedure and tissue processing

Surgery and subsequent tissue processing were done as outlined by Chaudhari et al. [16]. The animal handling and experimental protocol used in this study were approved by the Animal Ethics Committee of the KU Leuven and were performed according to the Belgian national legislation concerning the protection and wellbeing of animals (Approval ID: P122/2008). The study has used 26 mature New Zealand white rabbits, which have received four implants on the medial side of each proximal tibia. Double-stepped cavities (Ø 4 mm with a smaller inner cavity of Ø 2 mm with a depth of 0.5 mm) were prepared exclusively in the cortical bone by drilling. A standardized blood supply to the cavity during healing is ensured by a central perforation (Ø 0.5 mm) from the base of the cavity to the bone marrow. Sterilized implants were positioned into the outer cavity and fixed by a titanium osteosynthesis plate and two titanium osteosynthesis screws (Nobel Biocare, Sweden) to ensure a stable fixation. An implantation period of 2 and 4 weeks has been imposed and the implantation periods and samples were randomized over tibia as well as animals. Afterwards, animals were sacrificed and samples were harvested en-bloc, fixed in a formalin solution, dehydrated in increasing alcohol concentrations, and embedded in methylmethacrylate. Cross-sections perpendicular to the implant were prepared using a microtome diamond saw (Leica SP 1600, Leica Microsystems, Germany). Histomorphometry was done either by transmission light microscopy or BSE-SEM imaging. For transmission light microscopy, sections were ground to a thickness of ~ 30 µm using a micro-grinding system (Exakt 400 CS, Exakt, Germany) and surface stained with a combination of Stevenel's blue and Von Gieson's picrofuchsin. For SEM, samples were ground and polished followed by a gold coating.

2.4. Histomorphometry

The experimental bone model has been described in [16] and different histomorphometrical parameters used are summarized here. Fig. 1 shows a SEM image of a representative cross-section of a bone/implant entity. In the central cavity, no pre-existing bone was present at the time of implantation, the amount of newly formed bone detected in that area after a certain period serves as

a measure for the bone regeneration potential of the coating. Therefore, the central cavity is denominated ‘bone regeneration area (BRA)’. At the periphery of the BRA, there was initially direct contact between the implant and the cortical bone, permitting to assess the bone response in direct contact with the implant material. This area is referred to as the ‘bone adaptation area (BAA)’.

Fig. 1.

SEM micrograph of a histological section schematically indicating the regions of interest for histomorphometrical analysis: bone regeneration area (BRA) and bone adaptation area (BAA).

Evaluation of the bone response outside the porous coatings has been analyzed by transmission light microscopy (Laborlux, Leica, Germany) in combination with image analysis software (Axiovision 4.0, Zeiss). For the bone in-growth into the porous coatings, transmission light microscopy did not give reliable results because of the small pore size. Therefore, high resolution BSE–SEM image analysis (CTAn, SkyScan NV, Belgium) was performed to assess the bone in-growth inside the porous coatings. Main histomorphometrical parameters measured by transmission light microscopy are thus BRA-500 (within the whole cavity area of 500 μm), BRA-100 (within the 100 μm layer adjacent to the titanium implant surface), BIC–BRA: the bone-to-implant contact (BIC) with respect to the diameter of the entire BRA, and BIC–BAA: the bone-to-implant contact with respect to the sum of lengths of both BAA regions. To accommodate for the variable bone density for different animals and even different positions within the tibia, all parameters were normalized to the bone density in a reference area aside from the trauma zone, representing the bone's natural density.

2.5. Data-analysis

All the data collected from the specimens (Table 1) were used as is, without normalization. The data from in vivo studies (Table 2) were processed as individual records for every implant (ten specimens were processed for every material category). Histomorphic parameters were normalized by the respective area (Fig. 1) and expressed in percentage. Every specimen data were entered into a data file as a single record, which contains all information. During the analysis and visualization, no assumptions about the data internal structure have been made (meta-analysis does not require hypotheses about normality of the distributions) [8] and [9]. Data visualization and multi-variate analysis were made using Grapheur 2.1 (Reactive Search Ltd., Italy) and modeFrontier 4.4 (ESTECO Ltd., Italy).

Table 2.

Key histomorphometrical parameters of the various implant materials given in Table 1. Deviations for values are standard deviations with assumption of normal distribution.

Sample	Two weeks		Four weeks	
	BRA	BIC–BRA	BRA	BIC–BRA
Etched cp Ti	18.02 ± 8.86	11.24 ± 14.08	47.51 ± 17.49	25.51 ± 20.24
Anodised cp Ti	17.76 ± 12.77	6.05 ± 10.93	49.88 ± 16.19	22.30 ± 16.54
Anodised cp Ti → MBAG	15.53 ± 12.80	7.87 ± 19.48	52.48 ± 12.40	31.02 ± 27.72
EPD Ti (P)	19.44 ± 9.82	10.10 ± 10.62	41.44 ± 20.23	22.65 ± 14.87
EPD Ti (P_Vm)	19.80 ± 11.73	3.92 ± 7.19	39.95 ± 18.34	39.73 ± 21.20
EPD Ti (P) → HT	24.78 ± 11.49	15.65 ± 19.70	50.64 ± 18.61	29.75 ± 17.50
EPD Ti (P) → MAO	34.37 ± 18.02	12.97 ± 22.36	57.58 ± 16.63	22.87 ± 16.92
EPD Ti (P) → SGBAG	30.17 ± 7.20	6.54 ± 5.33	56.07 ± 9.88	6.84 ± 26.88

3. Results

3.1. Surface and bulk characterization

The surface parameters of porous and non-porous titanium implants were analyzed first from the point of view of their correlations. It was shown earlier by the authors [1] that some of the parameters are intrinsically linked (e.g. roughness Ra and Rz were clearly correlated). A similar trend is observed here as well (Fig. 2) since higher Sa parameter is expected to be associated with higher Sz. They are however not linked to texture (Str, size of points in Fig. 2) or developed surface area (Sdr, color of points in Fig. 2) ratios. Increased porosity affects the most the interconnecting pore channel mean size (IPC mean, Fig. 3), but not its lowest and highest values (Table 1). There is also less correlation between the porosity and roughness Sz. No correlations were found between wetting angle and porosity or roughness, as imposed surface treatments (HT, MAO or bioactive glass) make any type of implant very hydrophilic, overriding possible effects which would be seen on non-treated materials [1].

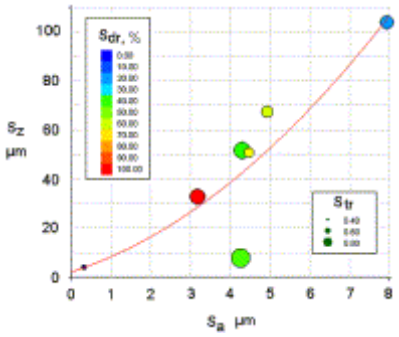

Fig. 2.

Dependence of surface parameters (Sz vs. Sa) with texture aspect ratio Str and surface developed ratio Sdr, all specimens (Table 1).

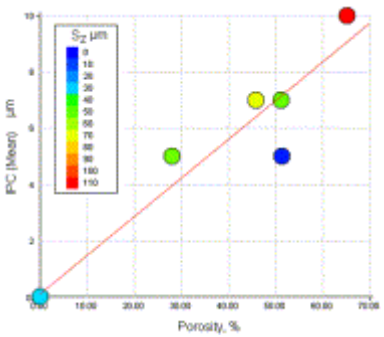

Fig. 3.

Dependence of the interconnection pore channel mean size vs. porosity and roughness (color scale).

3.2. Histomorphometry

The summary of the BRA and BIC parameters for two and four weeks of implantation is shown in Table 2. Here BRA has been averaged between 500 and 100 µm regions, as it was shown also earlier [1] that these two parameters are closely correlated. In Table 2 also standard deviations for the parameters are shown calculated with the assumption of the normal distribution of BRA and BIC–BRA values. As might be seen, in several cases standard deviations are higher than the mean values of the parameters and thus the conventional statistical conclusion might be difficult to justify. For example, for anodized Ti after 2 weeks of implantation BIC–BRA is 6 ± 11% which does not assure the bone-to-implant contact value to be a reliable parameter.

These data are plotted in Fig. 4 for BRA vs. BIC–BRA for all specimens shown by different implantation times (Fig. 4, a) and by specimen category (Fig. 4, b). From the first figure it is seen that BIC–BRA does not really change with increased implantation time — if some BIC values have been achieved at 2 weeks, only minor improvement follows after 4 weeks, no matter which specimen type was used (treated or not, porous or not). Fig. 4, b shows the same data but now explicitly by specimen categories. It is seen here that non-porous specimens are closely clustered (square points) for both 2 and 4 weeks of implantation times and there is no visible effect of etching, anodizing or BAG addition to this type of surfaces. Therefore, roughness and wetting angle (hydrophilic degree) do not eventually affect BRA and BIC–BRA values, but they might have an impact on biomechanical implant fixation, which was not analyzed in this study. For porous implant surfaces, implantation time also clearly doubles BRA and BIC–BRA values, Fig. 4, b. However, it is difficult to make conclusions on the basis of Table 2 and Fig. 4 alone, as average values and their deviations might be visually misleading and data scatter impact is not evident for multi-dimensional datasets.

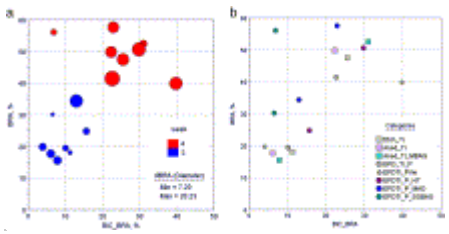

Fig. 4.

Histomorphometrical parameters (normalized) of BRA vs. BIC–BRA shown as for different implantation times (a) and for different specimen categories (b). For the last figure, note that non-

porous specimens (squares) are very close to each other for all treatment cases and implantation times.

For deeper analysis of these parameters, their original values (BRA500, BRA100, BIC–BRA and BIC–BAA) were fitted with different distributions. Fig. 5 shows examples BRA500 (over 500 μm thickness) for non-porous (a) and porous (b) specimens. Both cases have a very good fit with beta-distribution, but not with normal Gaussian.

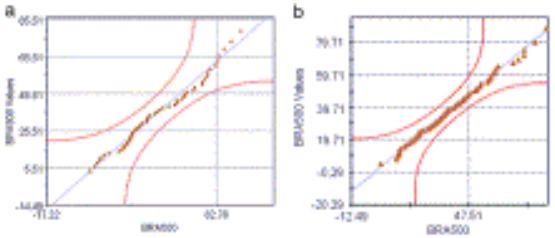

Fig. 5.

Distribution analysis of BRA500 (over 500 μm thickness) for non-porous (a) and porous (b) specimens. Both cases have a very good fit with beta-distribution (red quartile lines are possible outliers limits).

Fig. 6 presents cumulative probability example for BRA100 parameter for porous specimens. As can be seen, non-modified EPD Ti coatings (P and P_Vm) have close probabilities, following by hydrothermally treated (HT) material. Bioactive glass modified coating (SGBAG) has a little better slope, but the difference is small and might not have significance. Micro-arc oxidation (MAO) has the lowest probability of getting high BRA100 values by 20–30% vs. EPD Ti P or P_Vm (Fig. 6).

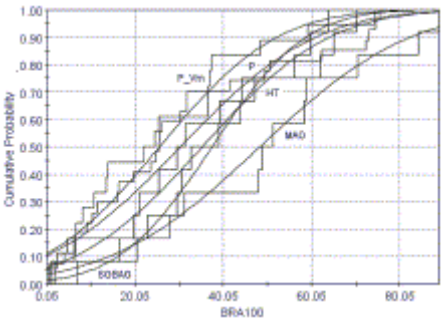

Fig. 6.

Cumulative probability of BRA100 parameter for porous specimens (specimen data from Table 1).

Fig. 7 combines the overall Student effects of the specimen parameters (Table 1) on BRA 500 and BIC–BRA values for both implantation times. One may see that wetting angle (hydrophilic ability) has the most valued share, highest for BIC–BRA. Surface roughness and morphology (Sa and Str) altogether have the second importance, followed by either pore size (for BRA) or porosity (for BIC–BRA). One however must remember that these parameters are not independent from each other (Fig. 2 and Fig. 3), so conclusions which could be yielded using such data of Fig. 7 should be considered with care.

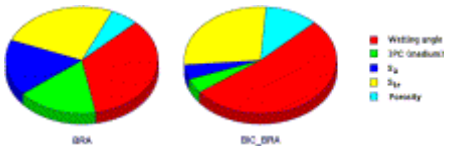

Fig. 7.

Overall Student factor analysis of specimen parameters on BRA500 and BIC–BRA values (all implantation times).

Fig. 8 plots box–whisker analysis of BRA500 and BIC–BRA for porous specimens, again for both implantation times. One may see that HT and MAO specimens represent an advantage for BRA500 vs. original (untreated) EPD Ti (P) or P/Vm mixture, with SGBAG showing slightly worse behavior (the densest half is lower than for HT and MAO cases), Fig. 8, a. For the BIC–BRA parameter, HT specimens are better than any others, with the worst data shown by SGBAG, Fig. 8, b.

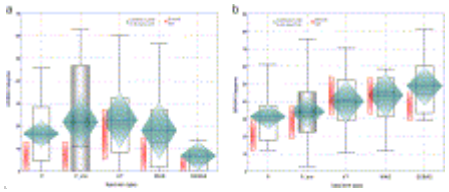

Fig. 8.

Box–whisker plots of the BRA500 (a) and BIC–BRA (b) parameters for porous specimens.

Also to visualize effect of the most critical factors (Fig. 7) on BRA and BIC–BRA values, they have been plotted vs. wetting angle, porosity and roughness (Fig. 9). As might be seen from Fig. 9, a, non-porous specimens are not really improving BRA500 values with more hydrophilic treatment for two weeks, but situation changes after four weeks of implantation (blue points at the top of the plot area). On the contrary, porous specimens have evident benefits when they are hydrophilic at both two and four weeks of implantation times. The BIC–BRA parameter has less pronounced dependence in the same coordinates (Fig. 9, b), and the data for four weeks (upper points in the plot) are almost inheriting their locations from two weeks of implantation time data (points located at the bottom half of the plot). However, as noted earlier, it would be improper to assess preferential specimen based on one or two plots like Fig. 9.

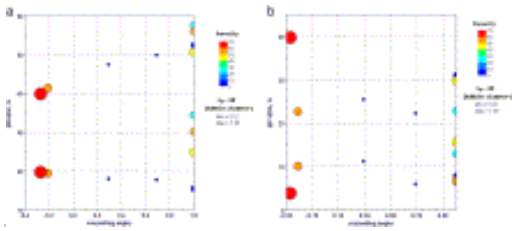

Fig. 9.

4D plot (X-axis: cosine of the wetting angle, Y-axis: BRA500 (a) or BIC–BRA (b), bubbles diameter: roughness Sa, µm, color scale: porosity) for all specimens and implantation times (bubbles of higher position are for 4 weeks and with lower position for 2 weeks).

For the selection of the “best” specimen used in this study, many parameters have to be assessed altogether. Mathematically it might be expressed in building a multi-dimensional plot and selecting one with the best values. Here one also should consider, which time scale would be appropriate: is it desirable that BRA or BIC–BRA are higher at the beginning (e.g. 2 weeks) or should one also target the maximal values after longer implantation time? This selection is further constrained by biomechanical requirements, as some implants might require better mechanical contact than others, so porosity and roughness might be fixed within certain limits.

The conclusion which might be drawn in this case indicates that for non-porous specimens there are little differences, but a BAG coated surface might perform somewhat better, especially at longer timescale. For porous specimens, the opposite seems to hold, as BAG-treated specimen behaves worse than others, especially vs. untreated EPD Ti (P and Vm), HT- and MAO-treated specimens. Hydrothermally treated EPD Ti (HT) has shown rather stable data for all implantation times for all parameters, and it might be recommended as a good compromise if the optimum balance is being sought between all these histomorphometrical values.

It is interesting to compare the key parameters of this EPD Ti specimens with those evaluated earlier [1] using in vitro tests. For maximal expected osteointegration, the results [1] recommended roughness Ra < 5 μm, titania layer thickness < 100 nm, total porosity of 30–50% with interconnecting pore channel mean size 2–7 μm. All porous specimens (Table 1) have such or similar roughness, less have similar channel size, but only one series was treated to form titania layer (EPD Ti (P) → HT, Table 1). These specimens have indeed been performing better than others, as shown above. It might be also seen that specimens with practically similar topology (all EPD Ti (P)) and low wetting angle (achieved however by different treatments) behaved also differently in vivo: BAG coating was less successful in porous structures than HT-TiO2. One of the possible reasons might be in chemistry of the resorption process — titania remains relatively inert in pores whereas BAG reacts with the biological environment, leading to local increase of pH which might be restricting factor for bone ingrowth if the liquid exchange in pores is not sufficiently fast. This assumption could be indirectly supported by the fact that BAG coating works reasonably well on non-porous specimens surfaces where there is no such limitation.

4. Conclusions

Several porous and non-porous titanium substrates have been studied in vivo from the point of view of their osteointegration vs. variations in porosity, pore topology, roughness and hydrophilic behavior. Key histomorphometrical parameters such as new bone formation in the regeneration area, bone adaptation area and bone-to-implant contact were determined after 2 and 4 weeks of implantation in rabbit animal model and correlated with materials parameters as well as previous in vitro data on bacterial attachment and cell reactions (proliferation and gene expression). A meta-analytical approach has been applied to the experimental data for assessing the effects and contributions of these factors, including total implantation time.

For non-porous specimens little differences have been observed, but thin BAG coating might behave somewhat better, especially at longer implantation times. For porous specimens, the opposite seems to hold, as BAG-treated specimen behaves worse behavior than others, whereas hydrothermally treated EPD Ti (P) → HT shows rather stable data for all implantation times for all parameters. It might be recommended as a good compromise if the optimum balance is being sought between all these histomorphometrical values. This behavior of porous HT specimens correlates well with the previous in vitro tests [1], which have proven to ensure also better condition for simultaneous

bacteria repelling and promotion of osteogenic cells reactions. The in vivo results also prove that hydrophilicity of an implant alone is not sufficient to “guarantee” positive results, as it might be achieved in different ways (e.g. by HT, MAO or BAG coatings). The latter does not provide good results in porous structures, possibly due to local pH increase as a result of BAG dissolution.

The results obtained suggest that more detailed analysis of the implant material parameters should be beneficial to combine with in vivo data to reveal “hidden” links and correlations between implant material and its realistic performance. It could also be advised that more details of the biomaterials have to be reported together with in vivo and clinical data — for example, listing of surface wettability only does not help if the means of its achievement would not be provided. Similar consistency is desirable for other physical parameters such as porosity topology or roughness, as there is always a risk of insufficient information when the implant processing data were confined into few values. Such limited data would make too high uncertainties in meta-analysis and eventually make it more difficult and less predictable.

Disclosure

Authors declare no competing or conflicting financial interests.

Acknowledgments

This work was supported by the 6th Framework of the Commission of the European Communities under project contract No. NMP3-CT-2006-026501 (MEDDELCOAT) and the Research Fund of KU Leuven under project IDO/06/013. Gratitude is extended to the Civil Engineering Department of KU Leuven and Dr. Ir. Bram Neirinck for mercury intrusion porosimetry measurements.

References

[1]

M. Gasik, L. Van Mellaert, D. Pierron, A. Braem, D. Hofmans, E. De Waelheyns, J. Anné, M.-F. Harmand, J. Vleugels

Adv. Healthc. Mater., 1 (2012), p. 117

[2]

P.C. Austin, L.J. Brunner, J.E. Hux

J. Eval. Clin. Pract., 8 (2002), p. 277

[3]

D.A. Berry

Stat. Med., 12 (1993), p. 1377

[4]

W.J.A. Dhert, C.C.P.M. Verheyen, L.H. Braak, J.R. de Wijn, C.P.A.T. Klein, K. de Groot, P.M. Rozingt

J. Biomed. Mater. Res., 26 (1992), p. 119

[5]

M. Svehla, P. Morberg, B. Zicat, W. Bruce, D. Sonnabend, W.R. Walsh

J. Biomed. Mater. Res., 51 (2000), p. 15

[6]

H.J. Rønold, S.P. Lyngstadaas, J.E. Ellingsen

Biomaterials, 24 (2003), p. 4559

[7]

M. Svehla, P. Morberg, W. Bruce, B. Zicat, W.R. Walsh

J. Arthroplasty, 17 (2002), p. 304

[8]

J. Branke, K. Deb, K. Miettinen, R. Słowinski (Eds.), Multiobjective Optimization, Interactive and Evolutionary Approaches, Springer, Berlin, Germany (2008)

[9]

R. Battiti, M. Brunato, F. Mascia

Reactive Search and Intelligent Optimization

Springer, Berlin, Germany (2008)

[10]

J. Quackenbush

Nat. Rev. Genet., 2 (2001), p. 419

[11]

B.S. Everitt

Medical Statistics From A to Z: A Guide for Clinicians and Medical Students

(2nd ed.)Cambridge Univ. Press, UK (2006)

[12]

B.R. Kirkwood, J.A.C. Sterne

Essential Medical Statistics

(2nd ed.)Blackwell Publ., UK (2003)

[13]

M. Gasik

EnginSoft Newsl., 3 (2010), p. 23

[14]

H. Celik, O. Gunduz, N. Ekren, Z. Ahmad, F. Oktar

J. Biomater. Nanobiotechnol., 2 (2011), p. 98

[15]

S.D. Puckett, E. Taylor, T. Raimondo, T.J. Webster

Biomaterials, 31 (2010), p. 706

[16]

A. Chaudhari, A. Braem, J. Vleugels, J.A. Martens, L. Naert, M.V. Cardoso, J. Duyck

PLoS One, 6 (2011), p. e0024186

[17]

A. Braem, T. Mattheys, B. Neirinck, J. Schrooten, O. Van der Biest, J. Vleugels

Adv. Eng. Mater., 13 (2011), p. 509

[18]

T. Mattheys, A. Braem, B. Neirinck, O. Van der Biest, J. Vleugels

Adv. Eng. Mater., 14 (2012), p. 371

[19]

B. Neirinck, T. Mattheys, A. Braem, J. Fransaer, O. van der Biest, J. Vleugels

Adv. Eng. Mater., 10 (2008), p. 246

[20]

N. Drnovšek, N. Daneu, A. Rečnik, M. Mazaj, J. Kovač, S. Novak

Surf. Coat. Technol., 203 (2009), p. 1462

[21]

S. Bouazza, E. Fuchs, A. Rosin, M. Willert-Porada

Mater. Sci. Forum, 631–632 (2010), p. 141

[22]

A. Braem, B. Neirinck, J. Schrooten, O. Van der Biest, J. Vleugels

Mater. Sci. Eng. C, 32 (2012), p. 2292

[23]

A. Wennerberg, T. Albrektsson

Int. J. Oral Maxillofac. Implants, 15 (2000), p. 331

Corresponding author at: Materials Science and Engineering Department, School of Chemical Technology, Aalto University Foundation, P. O. Box 16200, FIN-00076 AALTO, Finland.